Supporting Information: Ionic-like behavior of oppositely charged nanoparticles.

Alexander M. Kalsin, Anatoly Pinchuk, Bartlomiej Kowalczyk, Rafal Klajn, Bartosz A. Grzybowski*

Department of Chemical and Biological Engineering, and the Department of Chemistry, Northwestern University, 2145 Sheridan Rd., Evanston IL 60208

1. Materials and Methods.

1a. Synthesis of Nanoparticles. Dodecylamine (DDA)-coated gold and decanoic acid (DA)-coated silver nanoparticles were prepared according to a modified literature procedure (*S1*). For AuNPs, we used $HAuCl_4 \cdot 3H_2O$ instead of $AuCl_3$ and obtained smaller AuDDA particles: average sizes $\langle d \rangle$ were 3.5, 5.5 and 11.0 nm (instead of 4, 8 and 15 nm) and size dispersity was ~ 10-20%). AgDA NPs in toluene were stirred overnight to precipitate particles, whose average sizes were $\langle d \rangle$ = 5.3, 6.5 and 11 nm, with σ ~ 20%. The average sizes of the particles were estimated based on TEM images of at least 500 NPs of each type. Gold and silver NPs were functionalized with *N*,*N*,*N*-trimethyl(11-mercaptoundecyl)ammonium chloride (TMA), 11-mercaptoundecanoic acid (MUA), dihydrolipoic acid (DHLA) or unsymmetric disulfide $HO(CH_2)_{11}S\text{-}S(CH_2)_{10}COOH$ (SS). All ultrapure-grade thiols were obtained from ProChimia Surfaces (www.prochimia.com) and used as received.

1b. Ligand exchange on gold NPs. A toluene solution of DDA-capped gold particles (7 μmol/ml, 20 ml, 140 μmol) was quenched with 100 ml of methanol to give black precipitate. The supernatant solution with excess of capping agent and surfactant was decanted, and the precipitate was washed with methanol (50 ml), dissolved in toluene (100 ml), to which a thiol solution (140 μmol) in 10 ml of CH_2Cl_2 (MUA, DHLA, TMA) or in 30 ml of MeOH (SS) was added upon stirring. The precipitate of thiol-coated gold NPs was allowed to settle down, the mother-liqueur solution was decanted, and the solid was washed with CH_2Cl_2 (3×30 ml). The precipitate was then dissolved in 5 ml of methanol upon sonication. The AuMUA, AuDHLA and AuSS NPs were deprotonated with 25% methanolic solution of NMe_4OH (70 μL, 165 μmol), precipitated with acetone (30 mL), and washed with acetone (2×30 ml). The AuTMAs were precipitated with ethyl acetate (100 ml) and washed with CH_2Cl_2 and acetone. Finally, all the precipitates of thiol coated gold NPs were dried and dissolved in 13 ml of water to obtain ~10 mM solutions of NPs. The pH of the solutions was adjusted to ~11 with 0.2M solution of NMe_4OH.

1c. Ligand exchange on silver NPs. In a typical procedure, DA-coated silver NPs (30 mg, ~250 μmol) were dissolved in hot toluene (100 mL) and a solution of a thiol (250μmol) in 10 ml of CH_2Cl_2 was added. The dark brown precipitate was separated, and then washed (3×30 ml) with CH_2Cl_2. The precipitate was redispersed in 5 ml of methanol and precipitated with 30 ml of acetone, washed with

acetone and CH_2Cl_2 and then dried. The dried AgNPs were dissolved in 22 ml of deionized water to obtain ~10 mM solutions.

Both AuNP and AgNP solutions were subsequently used to prepare solutions of desired concentrations ranging from 0.2-5 mM (in terms of numbers of metal atoms).

1d. Estimation of NP Compositions. For silver NPs, the surface area occupied by a single thiol molecule on a silver nanoparticle was assumed to be the same as for gold nanoparticles, 21.4Å^2 (*S2*), since both gold and silver NPs have *fcc* crystal packing and their lattice constants are almost identical, namely 4.07Å and 4.08 Å, respectively).

1e. UV-Vis titration. The UV-Vis spectra were recorded on a Shimadzu UV-VIS spectrophotometer in the range 300-800 nm in an optical glass cell (1-10mm). The initial concentrations of aqueous NP (both Au and Ag) solutions ranged from 0.2 to 5 mM. In a typical experiment (procedures were analogous for other thiols and NPs), 2 mM solutions of AuMUA (400 μL, 0.8 μmol) were titrated in a stirred vial by adding 0.05-0.1 equivalent aliquots (20-40 μL) of 2 mM solutions of either AgTMA or AuTMA. The titrations were carried out in a stirred vial, and after each addition the solution was allowed to equilibrate for 5-10 min, and then transferred to a UV-Vis cell. The precipitation point was defined as the first point with the lowest absorption.

1f. Zeta potential measurements. The electrophoretic mobility of NPs was measured with Zeta/PALS particle sizer and surface potential analyzer (Brookhaven Instruments). The zeta potentials were derived from electrophoretic mobility values using Hückel approximation. For the zeta potential monitored titrations we used 0.2 mM – 5mM solutions of NPs, the same pHs of solutions as in the UV-Vis titrations: pH 10.8 for AuMUA and pH 6.8 for AuTMA. The pH measured after typical titration was ~ 9.5-10 ensuring that the carboxylic groups of the MUA ligands (pKa=6-8) remained fully deprotonated during the titration. Conductivity measurements showed that the ionic strength of AuMUA solution was higher (0.6mM), than that of AuTMA solution (~0.1mM), due to the presence of excess of base NMe_4OH.

1g. DLS titrations. DLS measurements were performed on Brookhaven BI-9000 instrument at 90 deg. scattering angle at 514 nm laser wavelength and 25 ^oC. In a typical experiment, 500 μL of 1 mM aqueous solution of nanoparticles of one polarity was titrated with 20-50 μL aliquots of 1 mM solution of oppositely charged NPs. The titrations were carried out in a stirred vial, and after each addition the solution was allowed to equilibrate for 7-8 min. The measurements were taken until the precipitation point was reached – this point (i) corresponded to the rapid increase in the average sizes of the aggregates and (ii) was confirmed by visual inspection of the sample and its UV-vis spectrum.

Figure S1a below illustrates this procedure for 11 nm AgTMA and AuMUA particles (effective hydrodynamic diameters are ~ 15 nm) and shows the steady increase in the average aggregate diameter during titration. As expected, the rate of this increase gradually slows down (since the addition of the

same number of NPs to a large aggregate has less effect on the aggregate size than addition to a small aggregate) before rapidly growing close to electroneutrality point.

Closer inspection of the aggregate size distributions (Fig. 1Sb-d) reveals that the aggregates that initially form (Fig. 1Sb) are ca. three NPs across – this observation is congruent with the core-and-shell structure shown in Fig. 2 in the main text. Furthermore, the "single" NPs (peak around 15 nm) disappears at around 20% of the titrant NPs added (Fig. 1Sc) suggesting that in the aggregates formed at this stage, each titrant NP is surrounded by five neighbors – this estimate agrees with the conclusion derived based on the electrodynamic modeling of the system (for details, see Kalsin et. al, *Nano Lett*. doi 10.1021/nl060967m, 2006).

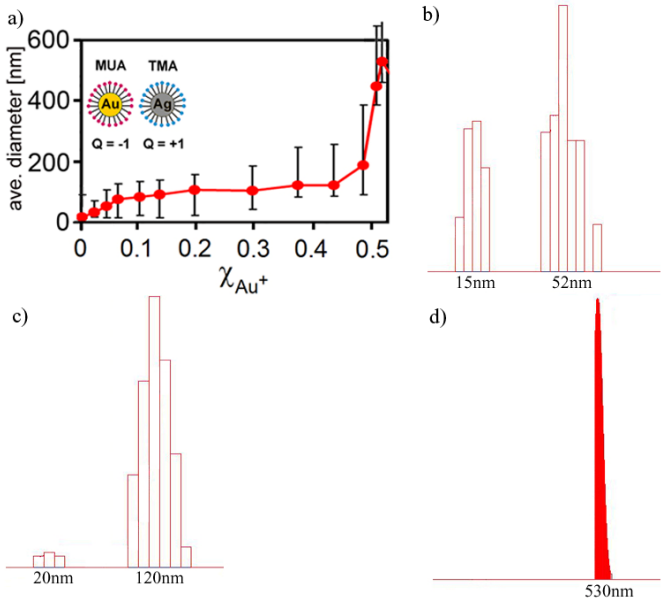

Fig. S1 (a) Avarage cluster size measured by DLS during titration of AgTMAs with AuMUAs. The histograms give distributions of aggregates' size for χ_{Au+} equal to **(b)** 0.025 (bimodal distribution with some free AgTMA particles still present); **(c)** 19% (when the free NPs begin to disappear) and **(d)** 52% (close to precipitation).

2. The characteristics of the UV-Vis spectra accompanying AgNP/AuNP titrations can be explained by the formation of "core-and-shell" aggregates in solution. When, during titration, AgNPs are added to the "sea" of AuNPs, the latter surround the former. Consequently, the wavelength of light reaching the Ag "core" is modulated upon passage through a "shell" of AuNPs (due to a different index of refraction).

The optical properties of the charged, core-shell clusters formed by discrete NPs are well approximated by those of "continuous," spherically symmetric, core-shell particles (*S3*). The intrinsic size effect in the optical absorption of silver and gold NPs due to limitations in the mean free path of the

conduction electrons inside the particles (*S4*) can be modeled using the size-corrected Drude approximation for the conduction electrons (*S5*) together with experimental data for the contribution of interband transitions (*S6*). The absorption cross section of a core-shell nanoparticle according to the Mie theory (*S7*) is then calculated as

$$C_{abs} = \frac{2\pi}{k^2}\sum_{j=1}^{\infty}(2j+1)\mathrm{Re}\{a_j + b_j\}\ ,\ \text{where}$$

$$a_j = \frac{\psi_j(y)[\psi_j'(n_2 y) - A_j\chi_j'(n_2 y)] - n_2\psi_j'(y)[\psi_j(n_2 y) - A_j\chi_j(n_2 y)]}{\xi_j(y)[\psi_j'(n_2 y) - A_j\chi_j'(n_2 y)] - n_2\xi_j'(y)[\psi_j(n_2 y) - A_j\chi_j(n_2 y)]},$$

$$b_j = \frac{n_2\psi_j(y)[\psi_j'(n_2 y) - B_j\chi_j'(n_2 y)] - \psi_j'(y)[\psi_j(n_2 y) - B_j\chi_j(n_2 y)]}{n_2\xi_j(y)[\psi_j'(n_2 y) - A_j\chi_j'(n_2 y)] - \xi_j'(y)[\psi_j(n_2 y) - B_j\chi_j(n_2 y)]},$$

$$A_j = \frac{n_2\psi_j(n_2 x)\psi_j'(n_1 x) - n_1\psi_j'(n_2 x)\psi_j(n_1 x)]}{n_2\chi_j(n_2 x)\psi_j'(n_1 x) - m_1\chi_j'(n_2 x)\psi_j(n_1 x)]},$$

$$B_j = \frac{n_2\psi_j(n_1 x)\psi_j'(n_2 x) - n_1\psi_j(n_2 x)\psi_j'(n_1 x)]}{n_2\chi_j'(n_2 x)\psi_j(n_1 x) - n_1\chi_j(n_2 x)\psi_j'(n_1 x)]}.$$

In these expressions, n_1 and n_2 are the refractive indices of, respectively, the core and shell relative to the surrounding medium, $x = kR_c$ and $y = kR_{sh}$, ψ, ψ' and ξ, ξ' are Riccati-Bessel functions and their derivatives; $k = 2\pi/\lambda$ where λ is the wavelength.

Qualitatively, this model predicts that the wavelength of light passing through the shell becomes shorter by a factor, which is determined by the shell's effective refractive index (cf. Fig. 2a) – as a result, the core is resonantly excited at a longer effective wavelength, $\lambda_{eff} = \lambda_{in.trinsic} n_{shell}$. This means that the effective wavelenght the AgNPs absorb is red-shifted to ~100 nm. Overall, the shell of AuNPs causes the AgNP SPR band to appear in the vicinity of the original Au SPR peak – this manifests itself in the apparent "extinguishing" of the silver band and "enhancement" of the composite band at around ~520-560 nm (Fig. S2).

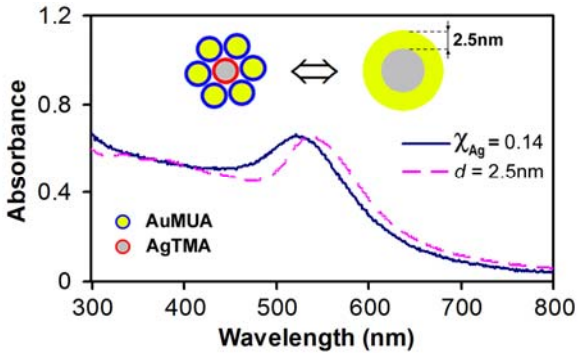

Fig. S2. Comparison of the experimental spectrum (solid line; note the absence of Ag SPR at 424 nm) characterizing titration of AuMUA (5.1nm) with AgTMA (4.8 nm) at χ_{Ag} = 0.14 with the calculated spectrum (dashed line) for the core-shell structures with an effective gold shell thickness of 2.5 nm. Since the calculated absorption cross-section of the 2.5 nm thick, continuous shell is six times that of an isolated gold nanoparticle, we estimate that the shell is composed of six AuNPs, which also agrees with χ_{Ag} = 0.14.

References

S1. Karpovich, D. S. & Blanchard, G. J. *Langmuir* **10**, 3315-3322 (1994).

S2. (a) Cooper, E. & Leggett, G. J. *Langmuir* **15**, 1024-1032 (1999). (b) Brewer, N. J. & Leggett, G. J. *Langmuir* **20**, 4109-4115 (2004).

S3. Hubenthal, F.; Ziegler, T.; Hendrich, C.; Alschinger, M.; Trager, F., *Eur. Phys. J. D* **34**, 165-168 (2005).

S4. Mie, G., *Annalen der Physik (Leipzig)* **25**, 377-445 (1908).

S5. Pinchuk, A.; Kreibig, U., *New J. Phys.* **5**, 151.1-151.15 (2003).

S6. Johnson, P. B.; Christy, R. W., *Phys. Rev. B* **6**, 4370-4379 (1972).

S7. Bohren, C. F.; Huffman, D. R., *Absorption and scattering of light by small particles*. Wiley Professional Paperback ed.; Wiley: New York, 1998; 'Vol.' p xiv, 530 p.

S8. Kalsin, A.M., Pinchuk, A., Paszewski, M., Schatz, G.C., Grzybowski, B.A., *Nano Lett.*, **2006**, doi 10.1021/nl060967m .